Newport Beach, CA, USA
inter-noise
1995 July 10-12 95

# A BOUNDARY ELEMENT APPROACH TO DETERMINE ACOUSTIC PROPERTIES OF HELMHOLTZ RESONATORS

Michihito TERAO and Hidehisa SEKINE

Kanagawa University, Rokkaku-bashi,
Kanagawa-ku, Yokohama-shi, Japan

## INTRODUCTION

The reactance and the resistance of a Helmholtz resonator govern its resonance frequency and absorption. The theoretical predictions of these acoustic properties had been reached the limit until 1950s. These theories give primarily the reactance of resonators with simple geometries. To predict both the reactance and the resistance of resonators with intricate geometries, we made an attempt to introduce a numerical approach to couple the acoustic-wave mode field with the thermal- and shear-wave mode fields in the close vicinity of the resonator wall. To confirm the effectiveness of this boundary element approach, we conducted experiments on a slit resonator attached to an impedance tube.

## ACOUSTIC PROPERTIES OF A HELMHOLTZ RESONATOR

A Helmholtz resonator is represented fully its acoustic properties by the specific acoustic impedance as a function of frequency, $z_{HR}$, which is defined as

$$z_{HR} = p_F / u_o = R + jX \qquad (1)$$

where $p_F$ and $u_o$ denote the sound pressure and the fluid velocity at the entrance of the aperture channel as shown in Fig. 1, $j^2 = -1$, and the real part R and imaginary part X of $z_{HR}$ are respectively the resistance and reactance of the resonator. The absorption coefficient of the resonator $\alpha$ is related to these as

$$\alpha = 4\hat{R} / \{(1+\hat{R})^2 + \hat{X}^2\} \qquad (2)$$

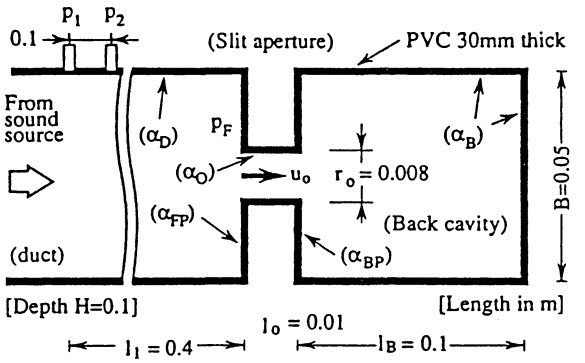


Fig. 1 Slit resonator used in the test.

in which $\hat{R} = R/(\rho c\sigma)$, $\hat{X} = X/(\rho c\sigma)$ and $\sigma = A_o/A_D$.
Here $\rho$ and c denote the density and sound velocity of the air, and $A_o$ and $A_D$ are the sectional area of the opening and the duct respectively. The absorption coefficient has been defined as the quotient between the power lost in the resonator and the power of the incident plane wave per unit area of the resonator front surface [1].

**Experimental Method.** Experiments were conducted on a slit resonator as shown in Fig. 1. To decompose the incident and reflected plane waves in the far field, the two-microphone method with impedance tube [2] was employed. From the far field pressures $p_1$ and $p_2$, the entrance pressure $p_F$ and velocity $u_o$ are derived in terms of the plane wave propagation model for the test duct, and then R and X of eq. (1) are given.

**Conventional Prediction Method.** The models for the reactance X and resistance R of a Helmholtz resonator are respectively given as

$$X = \omega M - K_B/\omega \qquad (3) \qquad\qquad R = 2R_v (l_o + \Delta l_R)/r_o \qquad (4)$$

where M and $K_B$ are the apparent mass per unit area and the stiffness of the air cavity, respectively, and are represented as

$$M = \rho\,(l_o + \Delta l_M) \tag{5}$$

$$K_B = \begin{cases} \rho c\sigma\omega \cot(\omega l_B/c) & \text{for distribution of plane waves in the cavity} \quad (6a) \\ \rho c^2 A_o/V_B & \text{for distribution of uniform pressure in the cavity.} \quad (6b) \end{cases}$$

In these equations, $\omega$ is the angular frequency, $l_o$ and $r_o$ denote the length and the width of the slit aperture, $V_B$ and $l_B$ represent the volume and the depth of the back cavity as shown in Fig. 1, $R_v$ is the resistance factor which will be described in the subsequent section, $\Delta l_M$ is the mass end correction for both sides of the aperture, and $\Delta l_M$ has been analytically given for the periodical slit [3] as shown in Fig. 1, as

$$\Delta l_M / r_o \approx \begin{cases} 0.95 & \text{for distribution of constant pressure in aperture cross-section} \quad (7a) \\ 1.0 & \text{for distribution of constant velocity in aperture cross-section.} \quad (7b) \end{cases}$$

For the resistance end correction $\Delta l_R$ we have $\Delta l_R/r_o \approx 2$ which was given empirically for circular holes [4].

## NUMERICAL ANALYSIS METHOD

To predict the far field pressures $p_1$ and $p_2$ and then R and X of a resonator, we employed a boundary element method for the acoustic-wave mode field and tried to give an appropriate boundary condition to take the wall viscosity and thermal effects into account.

**BE for Acoustic-wave Mode.** For the acoustic-wave mode field, discretizing the boundary surface into N boundary elements and exploiting the constant frequency version of the Kirchhoff-Helmholtz integral theorem, we have the relationships between the pressures and normal pressure gradients of all the boundary elements as,

$$\sum_{j=1}^{N} (G_{ij} q_j - H_{ij} p_j) = -f_i, \quad \text{for } i=1, 2, \cdots, N. \tag{8}$$

In this equation set, $p_j$ and $q_j$ denotes the pressure and its normal gradient, respectively, of the boundary element j, and are assumed to be constant over each element, and $G_{ij}$, $H_{ij}$ and $f_i$ are defined as

$$G_{ij} = \int_{\Gamma_j} g_{ij}\, d\Gamma \quad (9a), \qquad H_{ij} = \frac{\delta_{ij}}{2} + \int_{\Gamma_j} \frac{\partial g_{ij}}{\partial n} d\Gamma \quad (9b), \qquad f_i = \sum_{j=1}^{N^S} S_j g_{ij} \quad (9c)$$

in which $g_{ij}$ stands for the free space Green's function of the inhomogeneous Helmholtz equation. Specifically for a two dimensional case, it is given as

$$g_{ij} = -(j/4)\, H_0^{(2)}(kr_{ij}) \tag{10}$$

Here $H_0^{(2)}$ is the Hankel function of the second kind and of zero order, k is the wave number for the acoustic mode, i.e., $k = \omega/c$, $r_{ij}$ is the distance between the centroid point of the surface $\Gamma_i$ and an arbitrary point on the surface $\Gamma_j$, $\delta_{ij}$ is the Kronecker delta, and $S_j$ denotes the strength of point source j in the region, though no sound source of this kind was posed in the present work. The dimension of each boundary element taken here was 1 mm.

**Boundary Conditions for Thermal- and Shear-wave Modes.** For simplicity, we assume that each surface element has the prescribed acoustic property described as eq. (11a). For the acoustic admittance to match the acoustic-wave mode to the thermal- and shear-wave modes, we have an expression which contains the effective viscothermal admittance [5] which is written as the second term in eq. (11b):

$$\frac{q}{-j\omega\rho} = \beta(p - f_w) \tag{11a}$$

$$\beta = \frac{1}{z_w} + (1+j)\left\{\frac{R_h}{\rho^2 c^2} - \frac{R_v \nabla_{tan}^2}{\rho^2 \omega^2}\right\} \tag{11b}$$

where $q/(-j\omega\rho)$ is the outward normal velocity of the acoustic mode, $\beta$ and $f_w$ are the acoustic admittance and driving force of the surface element, and $z_w$ denotes the specific acoustic impedance of the solid wall. We assumed every surface as $f_w=0$ and $z_w=0$ except the surface of the test sound source. $R_v$ and $R_h$ are defined as

$$R_v/\rho c \equiv \omega d_v/2c \approx 2.0\sqrt{f}\times10^{-5} \quad (12a) \qquad R_h/\rho c \equiv \omega(\gamma-1)d_h/2c \approx 0.96\sqrt{f}\times10^{-5} \quad (12b)$$

in which $d_v=\sqrt{2\mu/\omega\rho}$ and $d_h=\sqrt{2\kappa/\omega\rho c_p}$ are the boundary layer thickness of the thermal- and shear-wave modes respectively, $\mu$ and $\kappa$ denote the viscosity and the thermal conductivity of the air, $c_p$ and $\gamma$ are the specific-heat coefficient at constant pressure and the specific-heat ratio of the air, and f denotes the frequency. The tangential Lapracian $\nabla^2_{tan}$ stands for the sum of the second derivatives with respect to the two coordinates tangential to the boundary surface, and $\nabla^2_{tan}p$ of each surface element was approximated in a finite difference expression by using the neighboring element pressures.

**Implicit Method.** Substituting $q_j$ of the eq. (8) by $p_{j+1}$, $p_{j-1}$ and $p_j-f_{wj}$, for each j by using the boundary conditions described by eq. (11), we can reconstruct eq. (8) into a set of N linear algebraic equations for N unknown pressures. Solving this equation system for these unknown pressures that involve the far field pressures at $p_1$ and $p_2$, R and X are given in the same way as was in the experiment.

**Explicit Method.** We studied also on possibility to utilize commercial numerical software as an alternative to the above implicit method. Under assumption of $q=0$, i.e., $z_w=\infty$, $R_h=0$ and $R_v=0$ in eq. (11), one can solve the equation system (8) for every $p_j$, but one can get only reactance X from the pressures $p_1$ and $p_2$. To obtain the resistance R by exploiting this pressure distribution, we have the expression [6] as

$$R=\int_{\Gamma_{HR}} I_n d\Gamma/(|u_o/\sqrt{2}|^2 A_o) \quad (13a)$$

$$I_n \approx R_v |u_{tan}/\sqrt{2}|^2 + R_h |p/\sqrt{2}\rho c|^2 \quad (13b)$$

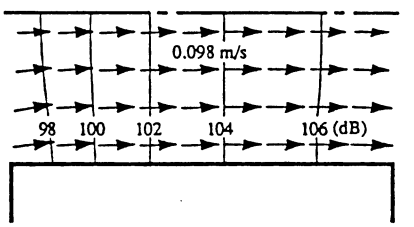


(A) Channel section of (a)

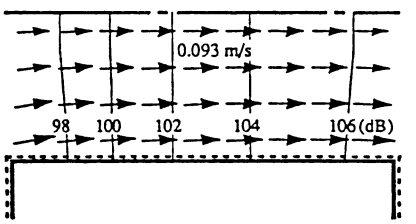


(B) Channel section of (b)

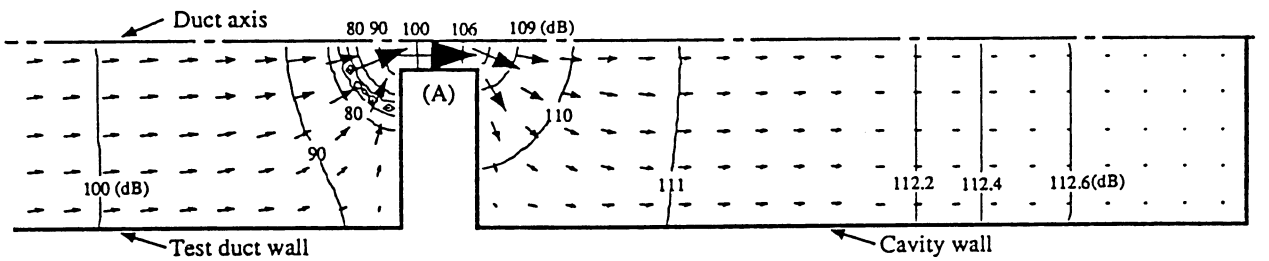


(a) Without viscothermal loss ($R_h=0$ and $R_v=0$).

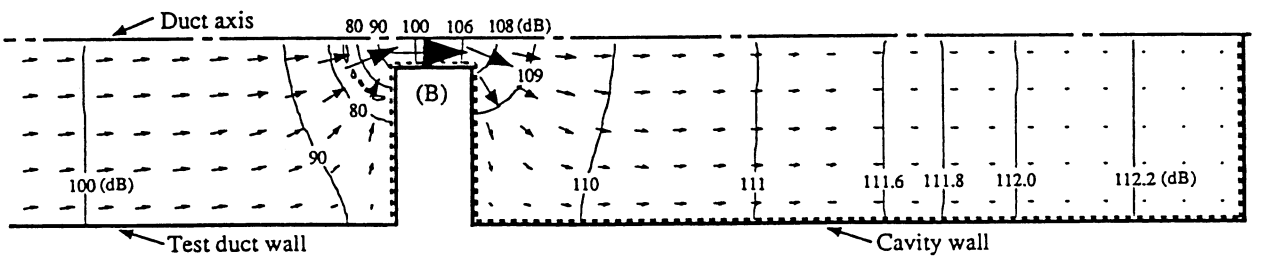


(b) With viscothermal loss ($R_v/\rho c = 2.0\sqrt{f}\times10^{-5}$ and $R_h/\rho c = 0.96\sqrt{f}\times10^{-5}$) on the wall with broken line (----).

Fig. 2 Pressure and velocity distribution around the slit resonator ($z_w=\infty$) by the numerical methods. Half side of the region about the axis of symmetry at resonance frequency 450 Hz is shown.

where $I_n$ indicates the net intensity towards the resonator wall $\Gamma_{HR}$, i.e., the energy dissipation from the acoustic-wave mode to the thermal- and shear-wave modes, and $u_{tan}$ denotes velocity tangential to the wall surface, which is given by taking the tangential gradient of the pressure. Eq. (13) is derived by approximating eq. (11), and an approximation of eq. (13) yields eq. (4) in turn.

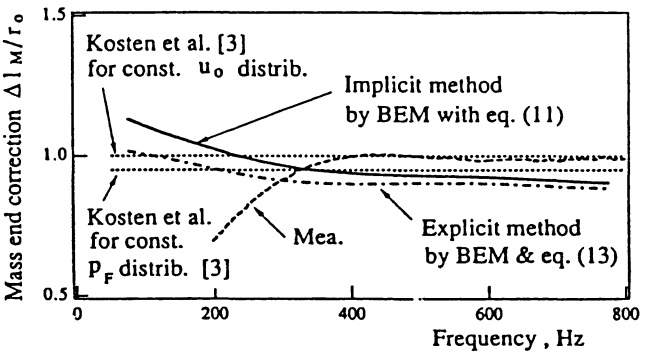


Fig. 3 Comparison of mass end corrections given by the methods.

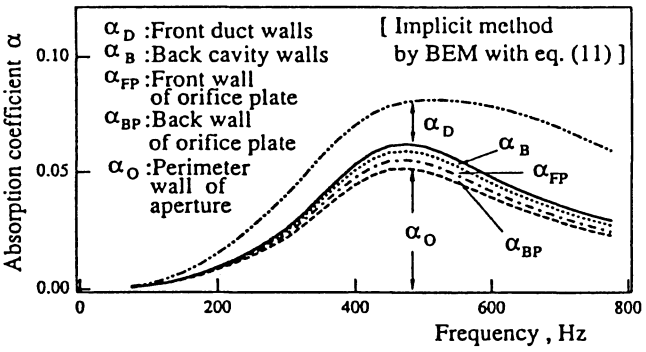


Fig. 4 Each wall contribution to absorption coefficient.

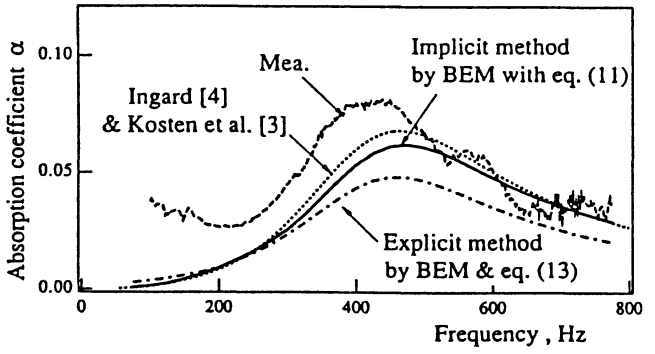


Fig. 5 Comparison of absorption coefficients given by the methods.

## TEST RESULTS

Fig. 2 compares the effect of the wall viscothermal loss on the pressure and velocity distributions in the numerical prediction. The discrepancies between (a) and (b) are not noticeable in this case of the small absorption coefficient. The pressure and velocity distributions in the cavity and at the aperture entrance are, strictly speaking, neither of plane waves nor uniform. This reduces slightly the effectiveness of the eq. (6) for $K_B$ and eq. (7) for $\Delta l_M$. However in the conventional prediction method in the subsequent comparison we employed eq. (6a) for $K_B$. Fig. 3 compares the methods for the mass end correction $\Delta l_M$. For measurement, the velocities are so small and tend to be erroneous that the results in the frequency region below the resonant frequency 450 Hz are not reliable. Except this frequency region, the discrepancies among the methods are not considerable. Fig. 4 shows each wall contribution, $\alpha_O$, $\alpha_{BP}$, $\alpha_{FP}$, $\alpha_B$ and $\alpha_D$ as indicated in Fig. 1, to the absorption coefficient obtained by the implicit numerical method. The absorption of the test duct, $\alpha_D$, is not negligible for a resonator with small absorption. Fig. 5 compares the methods on the absorption coefficient. For the measurement results, the contribution of the test duct absorption was excluded by $\alpha_D$ illustrated in Fig. 4. The measurement tends to give overestimation for such a resonator with small absorption coefficient less than about 0.06. The explicit numerical prediction gave somewhat underestimation of the absorption coefficient at the resonance frequency region in this case. By contrast, The implicit numerical prediction is thought to give reasonable absorption coefficient.

## CONCLUSIONS

We developed BE approach to predict the acoustic properties of a Helmholtz resonator by coupling the acoustic-wave mode field with the thermal- and shear-wave mode fields. This prediction method was tested on a slit resonator and gave reasonable prediction for the absorption coefficient due to the viscothermal loss at the resonator wall.

## REFERENCES

[1] L. Cremer et al, Principles and applications of room acoustics, p212, (Applied science publications, London, 1982)
[2] "Impedance and absorption of acoustical materials using a tube, two microphones, and a digital frequency analysis system, "ASTM standard E1050 (1985)
[3] "Sound absorption by slit resonators, "J.M.A. Smits and C.W. Kosten, Acustica, 1, 114-122, 1951.
[4] "On the theory and design of acoustic resonators, "K.U. Ingard, J. Acoust. Soc. Am., 25, 1037-1067 (1953)
[5] A.D. Pierce, Acoustics, Eq. (10-4.12), (Acoust. Soc. Am., New York, 1989)
[6] "Wall viscosity and heat conduction losses in rigid tubes," R.F. Lambert, J. Acoust. Soc. Am., 23, 480-481 (1951)